ESC European Society of Cardiology

European Heart Journal - Cardiovascular Imaging (2021) **22**, 950–958
doi:10.1093/ehjci/jeaa088

A head-to-head comparison of speckle tracking echocardiography and feature tracking cardiovascular magnetic resonance imaging in right ventricular deformation

Karim Taha[1,2*†], Mimount Bourfiss[1†], Anneline S.J.M. te Riele[1], Maarten-Jan M. Cramer[1], Jeroen F. van der Heijden[1], Folkert W. Asselbergs[1,3,4], Birgitta K. Velthuis[5‡], and Arco J. Teske[1‡]

[1]Department of Cardiology, University Medical Center Utrecht, Utrecht, the Netherlands; [2]Netherlands Heart Institute, Utrecht, the Netherlands; [3]Institute of Cardiovascular Science, Faculty of Population Health Sciences, University College London, London, UK; [4]Health Data Research UK and Institute of Health Informatics, University College London, London, UK; and [5]Department of Radiology, University Medical Center Utrecht, Utrecht, the Netherlands

Received 21 September 2019; editorial decision 8 April 2020; accepted 14 April 2020; online publish-ahead-of-print 27 May 2020

Aims Speckle tracking echocardiography (STE) and feature tracking cardiovascular magnetic resonance imaging (FT-CMR) are advanced imaging techniques which are both used for quantification of global and regional myocardial strain. Direct comparisons of STE and FT-CMR regarding right ventricular (RV) strain analysis are limited. We aimed to study clinical performance, correlation and agreement of RV strain by these techniques, using arrhythmogenic right ventricular cardiomyopathy (ARVC) as a model for RV disease.

Methods and results We enrolled 110 subjects, including 34 patients with definite ARVC, 30 preclinical relatives of ARVC patients, and 46 healthy control subjects. Global and regional RV longitudinal peak strain (PS) were measured by STE and FT-CMR. Both modalities showed reduced strain values in ARVC patients compared to ARVC relatives (STE global PS: $P < 0.001$; FT-CMR global PS: $P < 0.001$) and reduced strain values in ARVC relatives compared to healthy control subjects (STE global PS: $P = 0.042$; FT-CMR global PS: $P = 0.084$). There was a moderate, albeit significant correlation between RV strain values obtained by STE and FT-CMR [global PS $r = 0.578$ (95% confidence interval 0.427–0.697), $P < 0.001$]. Agreement between the techniques was weak (limits of agreement for global PS: ±11.8%). Correlation and agreement both deteriorated when regional strain was studied.

Conclusion RV STE and FT-CMR show a similar trend within the spectrum of ARVC and have significant correlation, but intermodality agreement is weak. STE and FT-CMR may therefore both individually have added value for assessment of RV function, but RV PS values obtained by these techniques currently cannot be used interchangeably in clinical practice.

Keywords deformation imaging • strain imaging • speckle tracking • feature tracking • right ventricle • ARVC

* Corresponding author. Tel: +31 (0)887555555; Fax: +31 (0)887555660. E-mail: k.taha-2@umcutrecht.nl

† The first two authors contributed equally to this article and are joint first authors.

‡ The last two authors contributed equally to this article and are joint senior authors.

© The Author(s) 2020. Published by Oxford University Press on behalf of the European Society of Cardiology.. This is an Open Access article distributed under the terms of the Creative Commons Attribution Non-Commercial License (http://creativecommons.org/licenses/by-nc/4.0/), which permits non-commercial re-use, distribution, and reproduction in any medium, provided the original work is properly cited. For commercial re-use, please contact journals.permissions@oup.com

Introduction

Speckle tracking echocardiography (STE) and feature tracking cardiovascular magnetic resonance imaging (FT-CMR) are advanced tools within the field of cardiac imaging, which both enable quantification of myocardial deformation.[1] Although these two techniques are used within different imaging platforms (i.e. echocardiography and CMR), both techniques use dedicated post-processing algorithms to identify markers in the myocardium and follow these markers throughout the cardiac cycle to track myocardial motion. The most fundamental parameter that is derived by these techniques is myocardial strain, which represents the amount of myocardial shortening during the cardiac cycle.

STE and FT-CMR are currently both applied to quantify right ventricular (RV) function in several diseases.[2–13] One of particular interest is arrhythmogenic right ventricular cardiomyopathy (ARVC). ARVC is an inheritable cardiomyopathy that is characterized by fibro-fatty replacement of the myocardium, typically of the RV.[14] Since the presence of structural heart disease identifies individuals who are at higher risk of life-threatening arrhythmias, echocardiography and CMR are sequentially performed in ARVC patients and their at-risk relatives.[15] STE and FT-CMR both enable detection of impaired RV strain in early stages of disease, which largely goes unnoticed by conventional imaging measurements.[2–8] These subclinical abnormalities have recently been associated with development of clinical disease progression, and therefore, RV strain analysis may improve screening protocols in relatives of ARVC patients.[5]

Since STE and FT-CMR are both applied in similar patients for measurement of RV strain, insight into the interchangeability of these measurements is of clinical relevance. STE and FT-CMR have been extensively compared in previous studies, but these studies mainly focused on left ventricular (LV) strain measurements.[16–18] In the present study, we aimed (i) to compare RV strain analysis by STE and FT-CMR with regard to clinical performance in ARVC and (ii) to study correlation and agreement between these techniques.

Methods

Study population

Subjects that were eligible for this study were patients with definite ARVC according to the 2010 Task Force Criteria (TFC) and relatives of ARVC patients (not fulfilling definite ARVC diagnosis) who were evaluated at the University Medical Center Utrecht between 2004 and 2018.[19,20] In this period, 297 unique subjects underwent echocardiography and 242 underwent CMR as part of routine clinical care. Relatives who underwent genetic testing but who were not found to carry the index mutation were excluded. Subjects who underwent both echocardiography and 1.5-T CMR within 1 month were included in the final study population, provided that the images were appropriate for RV strain analysis by both STE and by FT-CMR. A group of healthy non-athlete subjects who underwent echocardiography and 1.5-T CMR within 1 day for a previous study served as control group.[21] The control group was age- and gender-matched with ARVC relatives. This study was approved by the local institutional ethics committee and was performed according to the principles of the Declaration of Helsinki and the European General Data Protection Regulation.

Echocardiography and STE

All echocardiograms were obtained with Vivid 7 or Vivid E9 (GE Healthcare, Horten, Norway) according to a standardized protocol.[22] RV outflow tract dimensions were measured in the parasternal long-axis view and parasternal short-axis view, and fractional area change was measured in the apical four-chamber view.[19] Longitudinal strain analysis was performed offline with GE EchoPac version 202.39 (GE Healthcare, Horten, Norway) by two experienced observers who were blinded for clinical data and FT-CMR results. Inter- and intra-observer agreement was recently shown to be excellent: reported kappa values were 0.94 and 0.93, respectively.[5,6] The analyses were performed according to a previously published protocol.[22] In brief, a narrow-angle RV-focused recording from the apical four-chamber view was used.[23] Frame rates between 55 and 110 frames/s were accepted for deformation imaging. Onset of systole was set at the beginning of the QRS complex on the electrocardiogram (ECG). The endocardial border of the RV lateral wall was manually traced. The apical cap was not included in the region of interest. When necessary, the region of interest thickness was adjusted manually to include the RV myocardium or to exclude the pericardium. The region of interest was automatically divided into a basal, mid and apical segment. A representative example is shown in *Figure 1*.

CMR and FT-CMR

All CMR images were acquired using a 1.5-T scanner (Philips Medical Systems, Best, the Netherlands). RV dimensions and ejection fraction were measured on short axis (repetition time/echo time/flip angle 2.9/1.4/60°, matrix 192–256, field of view 320 mm, temporal resolution ≤50 ms, slice thickness 8 mm). Ventricular end-diastolic and end-systolic volumes were measured and corrected for body surface area. Longitudinal strain analysis was performed in the horizontal long axis using Medis Qstrain Software (Medis Medical Imaging Systems, version 3.1, Leiden, the Netherlands) by one experienced observer blinded for clinical data and STE results. Endocardial contours of the RV (from lateral to septal) were manually drawn during end-diastole and end-systole with subsequent automatic tracking during the cardiac cycle. Onset of systole was determined on the basis of ventricular volumes. The endocardial border was automatically segmented into seven regions of equal size; three segments in the lateral free wall (basal, mid, and apical), apical cap and three segments in the septal wall (basal, mid, and apical). A representative example is presented in *Figure 1*.

Strain parameters

All strain values in this study are reported as absolute values. With STE and FT-CMR, regional peak strain (PS) was derived from the basal, mid, and apical region of the RV lateral wall (*Figure 1*). The apical cap was not included in the analysis according to current recommendations.[23] The interventricular septum was not taken into account, because it is also considered to be part of the LV.[23] PS was defined as the maximum amount of myocardial shortening during the cardiac cycle, expressed in percent. Global PS was defined as the average PS of the three segments of the RV lateral wall. Global PS was only calculated when all three RV lateral wall segments were eligible for analysis by both modalities.

Vendor-independent analysis

The aforementioned analyses were performed with different software packages for STE and FT-CMR. To study the effect of software-dependence, we additionally measured global and regional PS in the RV free wall with a vendor-independent software package that can process both echocardiographic and CMR data for STE and FT-CMR analysis (TomTec Image Arena version 4.6, Unterschleissheim, Germany). This software package automatically determines onset of systole on the basis

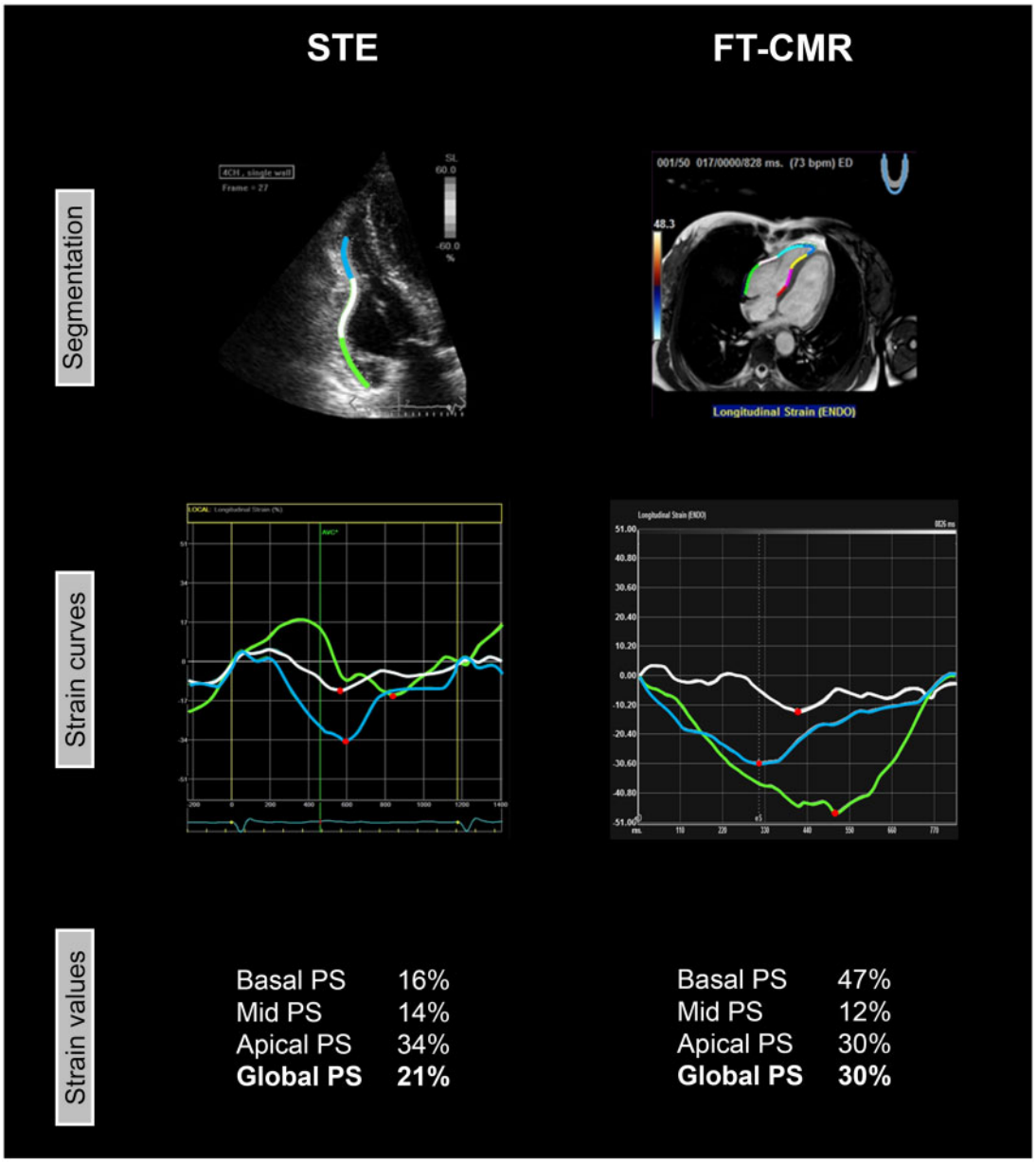

Figure 1 Representative example of RV analysis by STE and FT-CMR in one patient. The RV lateral wall was analysed with STE (left) and FT-CMR (right). In both techniques, the RV lateral wall was automatically divided in three segments (basal/green, mid/white, and apical/blue). From these three segments, PS was derived, which is defined as the maximum amount of myocardial shortening (red dots). Global PS is defined as the average PS from the three RV segments. FT-CMR, feature tracking cardiovascular magnetic resonance imaging; PS, peak strain; STE, speckle tracking echocardiography.

of ventricular volumes (i.e. frame/phase with largest RV area on echocardiography or CMR). The vendor-independent analysis was performed in a random selection of 30 subjects (10 ARVC patients, 10 ARVC relatives, and 10 controls).

Statistical method

Data are expressed as mean ± standard deviation (SD) or as median (interquartile range). Normal distribution was tested using the Shapiro–Wilk test. Significance of differences between three groups was calculated using a one-way analysis of variance or a Kruskal–Wallis test. Significance of differences between two groups was calculated using an independent Student's *t*-test or Mann–Whitney *U*-test. Binary data were compared using a Fischer's exact test. Bonferroni correction was applied in case of multiple testing (i.e. multiplication of obtained *P*-value by the number of tests). Direct comparison of strain values by STE and FT-CMR was performed by a paired *t*-test or a Wilcoxon signed rank test. For assessment of correlation, Pearson's *r* test was used. In case of non-linearity, Spearman's rank test was performed. Agreement between the

Table 1 Baseline characteristics

	ARVC patients ($n = 34$)	ARVC relatives ($n = 30$)	Control subjects ($n = 46$)	*P*-value
Age (years)	43.4 ± 17.9**	32.6 ± 16.8	27.3 ± 5.4	<0.001
Males	18 (53)	14 (47)	21 (46)	0.834
Pathogenic mutation	27 (79)	24 (80)		1.000
Desmosomal	23 (68)	16 (53)		0.307
Non-desmosomal	4 (12)	8 (27)		0.199
2010 TFC (points)	6 (4)*	2 (1)		<0.001
Structural TFC	25 (74)*	2 (7)		<0.001
Depolarization TFC	20 (59)*	5 (17)		0.001
Repolarization TFC	20 (59)*	3 (10)		<0.001
Arrhythmia TFC	30 (88)*	5 (17)		<0.001
Family history TFC	29 (85)*	30 (100)		0.253
Echocardiography				
RVOT-PLAX (mm)	35.4 (9.0)**	27.8 (9.0)	26.1 (5.6)	<0.001
RVOT-PSAX (mm)	36.5 (6.9)**	29.4 (5.4)	28.8 (4.0)	<0.001
FAC (%)	37.5 ± 11.0**	47.7 ± 7.0	45.2 ± 4.2	<0.001
CMR				
RV-EDV (mL/m^2)	116.3 (59.4)**	90.4 (23.6)*	99.8 (27.1)	<0.001
RV-ESV (mL/m^2)	63.2 (56.4)**	39.9 (16.5)*	47.3 (17.1)	<0.001
RVEF (%)	42.2 ± 12.6**	55.7 ± 6.8	53.3 ± 5.2	<0.001

Values are presented as mean ± SD, median (interquartile range), or *n* (%). An asterisk (*) indicates a statistical significant difference ($P < 0.05$) compared to the adjacent group at the right and a double asterisk (**) indicates a statistical significant difference compared to the two adjacent groups at the right. Statistical tests between subgroups are performed with a Bonferroni correction for multiple testing.
ARVC, arrhythmogenic right ventricular cardiomyopathy; EDV, end-diastolic volume; ESV, end-systolic volume; FAC, fractional area change; PLAX, parasternal long-axis view; PSAX, parasternal short-axis view; RV, right ventricular; RVEF, right ventricular ejection fraction; RVOT, right ventricular outflow tract; TFC, task force criteria.

two modalities was assessed by Bland–Altman analysis. The bias was calculated as the mean measurement difference between the two techniques (FT-CMR–STE), whereas 95% limits of agreement were calculated as twice the SD of the measurement difference. *P*-values of <0.05 were considered to indicate statistical significance. *P*-values between 0.05 and 0.1 were considered to be borderline significant. All statistical analyses were performed using SPSS Statistics for Windows version 23.0 (IBM Corporation, Armonk, NY, USA).

Results

Baseline characteristics

The study population consisted of 110 subjects, including 34 ARVC patients (31%), 30 ARVC relatives (27%) and 46 healthy control subjects (42%). Baseline characteristics are shown in *Table 1*. By design, ARVC relatives and control subjects were age- and gender-matched. ARVC patients were older than the other groups ($P < 0.001$). Gender was equally distributed between ARVC patients and the other groups ($P = 0.834$). The number of subjects carrying a pathogenic mutation was equal in ARVC patients and ARVC relatives [$n = 27$ (79%) vs. $n = 24$ (80%), $P = 1.000$]. ARVC relatives without a proven mutation were either relatives who did not undergo genetic testing ($n = 4$) or relatives of mutation-negative index patients ($n = 2$).

By design, all control subjects had echocardiography and CMR within 1 day. The timeframe between echocardiography and CMR was equal in ARVC patients and relatives (4 ± 8 days vs. 3 ± 6 days, $P = 0.115$).

By conventional measurements, echocardiography and CMR both showed increased RV size ($P < 0.001$) and decreased RV function ($P < 0.001$) in ARVC patients compared to ARVC relatives and control subjects (*Table 1*). RV size and RV function were within normal range by conventional measurements in ARVC relatives when compared with control subjects.[24] More conventional measurements are shown in Supplementary data online, *Table S1*.

Strain analysis

With STE, 315 segments (95%) were eligible for strain analysis; the basal segment was excluded in one subject, the mid segment was excluded in three subjects and the apical segment was excluded in 11 subjects. With FT-CMR, 328 segments (99%) were eligible for strain analysis; the mid segment was excluded in one subject and the apical segment was excluded in another. Overall, higher PS values were seen with FT-CMR compared to STE (*Table 2*). Furthermore, a wider range of PS values was seen with FT-CMR compared to STE (Supplementary data online, *Figures S1–S4*).

With STE, mean PS in the apical segment was higher than in the basal segment (27.5 ± 5.5% vs. 20.8 ± 6.1%, $P < 0.001$). With FT-CMR, this gradient was reversed; mean PS in the basal segment was higher than in the apical segment (38.0 ± 9.1% vs. 32.6 ± 11.8%, $P < 0.001$).

Table 2 Mean strain values, correlation and agreement

	Global PS ($n = 96$)	Basal PS ($n = 109$)	Mid PS ($n = 106$)	Apical PS ($n = 98$)
STE PS (%)	24.3 ± 5.2	20.8 ± 6.1	24.7 ± 5.8	27.5 ± 5.5
FT-CMR PS (%)	33.2 ± 7.1	38.0 ± 9.1	29.0 ± 11.3	32.6 ± 11.8
Rho (95% CI)	0.578 (0.427–0.697)*	0.490 (0.333–0.620)*	0.399 (0.159–0.497)*	0.261 (0.066–0.436)*
Bias (%)	8.8	17.5	4.2	4.8
Limits of agreement (%)	±11.8	±16.2	±21.6	±23.4

Strain measurements are presented as absolute values (mean ± SD). An asterisk (*) indicates a significant correlation ($P < 0.05$).
FT-CMR, feature tracking cardiovascular magnetic resonance imaging; PS, peak strain; STE, speckle tracking echocardiography.

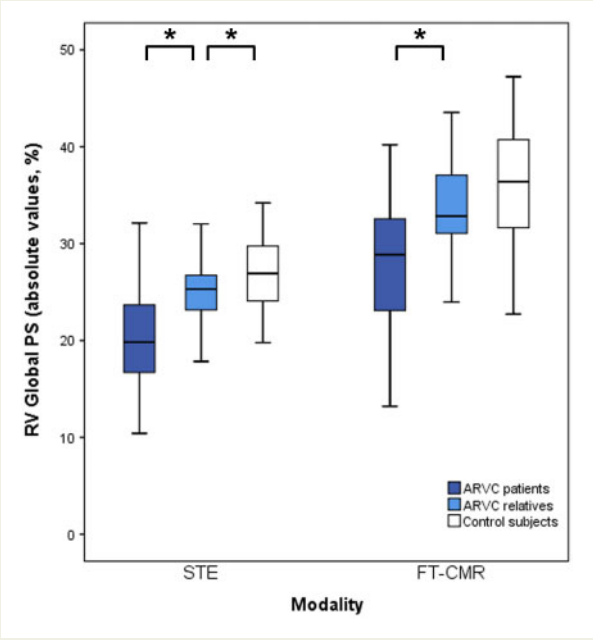

Figure 2 Global RV PS in different clinical stages by STE and FT-CMR. With STE (left) and FT-CMR (right), similar differences of RV strain values are seen between ARVC patients, ARVC relatives and healthy controls. An asterisk (*) indicates a statistically significant difference ($P < 0.05$). ARVC, arrhythmogenic right ventricular cardiomyopathy; PS, peak strain; RV, right ventricular.

While with STE the lowest PS values were found in the basal segment, FT-CMR showed the lowest PS values in the mid segment.

Clinical performance

Global strain

STE and FT-CMR both showed significantly lower global PS values in ARVC patients compared to ARVC relatives (*Table 3*, *Figure 2*): global PS with STE was 19.7 ± 5.7% in ARVC patients and 25.1 ± 3.4% in ARVC relatives ($P < 0.001$), global PS with FT-CMR was 27.9 ± 6.7% in ARVC patients and 33.6 ± 5.2% in ARVC relatives ($P < 0.001$). When comparing ARVC relatives with control subjects, STE and FT-CMR both showed reduced global PS in ARVC relatives, which was statistically significant with STE and borderline statistically significant with FT-CMR (*Table 3*, *Figure 2*): global PS in control subjects was 27.1 ± 3.5% ($P = 0.042$) with STE and 36.4 ± 6.0% with FT-CMR ($P = 0.084$).

Regional strain

STE showed lower strain values in ARVC patients compared to ARVC relatives in the basal segment ($P < 0.001$), in the mid segment ($P < 0.001$), and in the apical segment ($P = 0.052$) (*Table 3*). FT-CMR also showed lower strain values in ARVC patients compared to ARVC relatives in the basal segment ($P = 0.030$) and in the mid segment ($P = 0.034$) (*Table 3*). When comparing ARVC relatives with control subjects, STE showed lower strain values in ARVC relatives in the basal segment ($P = 0.078$) and in the mid segment ($P = 0.040$). This was also seen with FT-CMR in the basal segment ($P = 0.070$) and in the mid segment ($P = 0.070$).

Correlation and agreement

Global strain

Correlation between STE and FT-CMR for global PS was moderate [$r = 0.578$ (0.427–0.697), $P < 0.001$]. Bland–Altman plots for global PS are displayed in *Figure 3*. For global PS, bias between STE and FT-CMR was 8.8% and limits of agreement were ±11.8%. Limits of agreement for global PS were comparable for ARVC patients, ARVC relatives, and control subjects (±13.0, ±10.6 and ±11.6, respectively, Supplementary data online, *Figure S5*).

A subgroup analysis was performed for subjects who had echocardiography and CMR on the same day ($n = 81$). Correlation and agreement did not improve in this subgroup (Supplementary data online, *Table S2*), nor did correlation and agreement improve when STE and FT-CMR were performed with a similar software package (Supplementary data online, *Figure S9* and *Table S3*).

Regional strain

Correlation was weaker for regional PS than for global PS (*Table 2*). Bland–Altman plots for regional PS in the basal, mid, and apical segments are displayed in *Figure 3*. Limits of agreement were wider for regional PS than for global PS (basal segment ±16.2%; mid segment ±21.6%; apical segment ±23.4%). Limits of agreement for regional PS were comparable for ARVC patients, ARVC relatives and control subjects (Supplementary data online, *Figures S6–S8*). Consistently higher PS values were measured with FT-CMR in the basal segment compared to STE (lower limit of agreement: 1.3%, upper limit of agreement: 33.7%).

Table 3 Comparison of measurements in different clinical stages

	STE					FT-CMR				
	ARVC patients ($n = 34$)	ARVC relatives ($n = 30$)	Control subjects ($n = 46$)	*P*-value patients-relatives	*P*-value relatives-controls	ARVC patients ($n = 34$)	ARVC relatives ($n = 30$)	Control subjects ($n = 46$)	*P*-value patients-relatives	*P*-value relatives-controls
Global PS (%)	19.7 ± 5.7	25.1 ± 3.4	27.1 ± 3.5	<0.001	0.042	27.9 ± 6.7	33.6 ± 5.2	36.4 ± 6.0	<0.001	0.084
Basal PS (%)	15.0 ± 6.5	22.0 ± 3.7	24.0 ± 3.8	<0.001	0.078	32.3 ± 9.4	37.7 ± 8.3	41.8 ± 7.6	0.030	0.070
Mid PS (%)	19.7 ± 6.0	25.2 ± 3.5	27.7 ± 4.3	<0.001	0.040	22.2 ± 10.9	28.5 ± 9.5	33.7 ± 10.4	0.034	0.070
Apical PS (%)	24.2 ± 6.8	27.3 ± 4.0	29.6 ± 4.0	0.052	0.110	29.3 ± 12.7	34.8 ± 9.3	33.7 ± 12.5	0.114	1.000

Strain measurements are presented as absolute values (mean ± SD).
ARVC, arrhythmogenic right ventricular cardiomyopathy; FT-CMR, feature tracking cardiovascular magnetic resonance imaging; PS, peak strain; STE, speckle tracking echocardiography.

Discussion

The present study is among the first to compare RV strain values derived by STE and FT-CMR. We found that STE and FT-CMR show a comparable trend of RV strain values among ARVC patients and relatives. This led to a significant correlation between the modalities, but suboptimal agreement. Based on our findings, we can neither recommend using STE and FT-CMR interchangeably, nor can we provide a correction factor to correct the bias between the two different techniques.

Clinical utility in ARVC

STE and FT-CMR are both increasingly applied to quantify global and regional RV deformation in ARVC.[2–9] In our study, both techniques independently showed comparable differences between subgroups in ARVC. Both techniques showed significant differences between ARVC patients and relatives of ARVC patients (who do not fulfil ARVC diagnosis) with both global and regional RV strain. Interestingly, both techniques also found lower strain values in at-risk relatives than in healthy control subjects. These abnormalities were not picked up by conventional imaging measurements, which supports the hypothesis that conventional imaging modalities lack sensitivity to detect early structural signs of ARVC. The differences between ARVC relatives and healthy control subjects were found to be statistically significant with STE and borderline statistically significant with FT-CMR, which might suggest that STE is more sensitive for a subtle decrease of RV PS values than FT-CMR.

Correlation and agreement

Previous studies comparing RV STE and RV FT-CMR showed a moderate correlation between these techniques ($r = 0.45$ and $r = 0.56$, respectively).[10,11] Previous studies investigating agreement between RV STE and RV FT-CMR are scarce and of small sample size. Kempny *et al.*[12] performed RV strain analysis by STE and FT-CMR in a cohort of 28 adult patients with repaired tetralogy of Fallot (TOF) and 25 healthy controls, and reported limits of agreement of ±8.3% for RV global longitudinal PS. Furthermore, Padiyath *et al.*[13] compared STE and FT-CMR in 20 patients with TOF and 20 control subjects, and reported comparable limits of agreement for RV global longitudinal PS of ±8.5%. The wide limits of agreement in both aforementioned studies already suggested that strain values derived by STE and FT-CMR cannot be used interchangeably in clinical practice. However, since these studies were both performed in patients with congenital heart disease and subsequent RV remodelling (i.e. RV hypertrophy), these results cannot be compared to the results of the present study.

In accordance with the previous studies, we found a moderate but significant correlation between STE and FT-CMR. We found inter-modality agreement between STE and FT-CMR for RV strain analysis to be poor. FT-CMR tended to show higher RV strain values (particularly in the basal segment). The magnitude of the global and regional RV strain values that were found with FT-CMR were not reported before by the reference standard sonomicrometry.[25,26] Remarkably, we observed reversed gradients of PS from the basal to the apical segment of the RV free wall in the two techniques (which is in accordance with previous studies).[4,21] Our results confirm that global and regional RV strain measurements by STE and FT-CMR currently cannot be used interchangeably on an individual level.

The following factors may have contributed to the observed inter-modality differences.

- STE and FT-CMR are based on similar physical principles, but the techniques use different markers to quantify myocardial motion. In STE, 'speckles' are followed throughout the cardiac cycle, which are distinct acoustic backscatters that result from interference of ultrasound waves with the myocardium. CMR images do not have such scatters, and instead FT-CMR algorithms use 'features' which are anatomic elements that are identified along the cavity-myocardial interface. It remains unknown whether the motion of speckles and features are equally representative for RV myocardial deformation.
- The difficulty to match myocardial segments between echocardiography and CMR due to different scanning angles is a known source of inter-modality variation. This is particularly true for the RV because of its complex geometry and anatomical position in the chest. In this study, we aimed to analyse the RV lateral wall with both techniques, but slight differences in slice position between the two modalities are inevitable and cannot be excluded.
- Echocardiography and CMR are known to differ in spatial and temporal resolution. While the signal-to-noise ratio is relatively high in CMR, echocardiography may be limited by suboptimal acoustic windows and thus suboptimal endocardial delineation, particularly when imaging the RV. This is illustrated by a higher number of excluded segments in echocardiography than in CMR

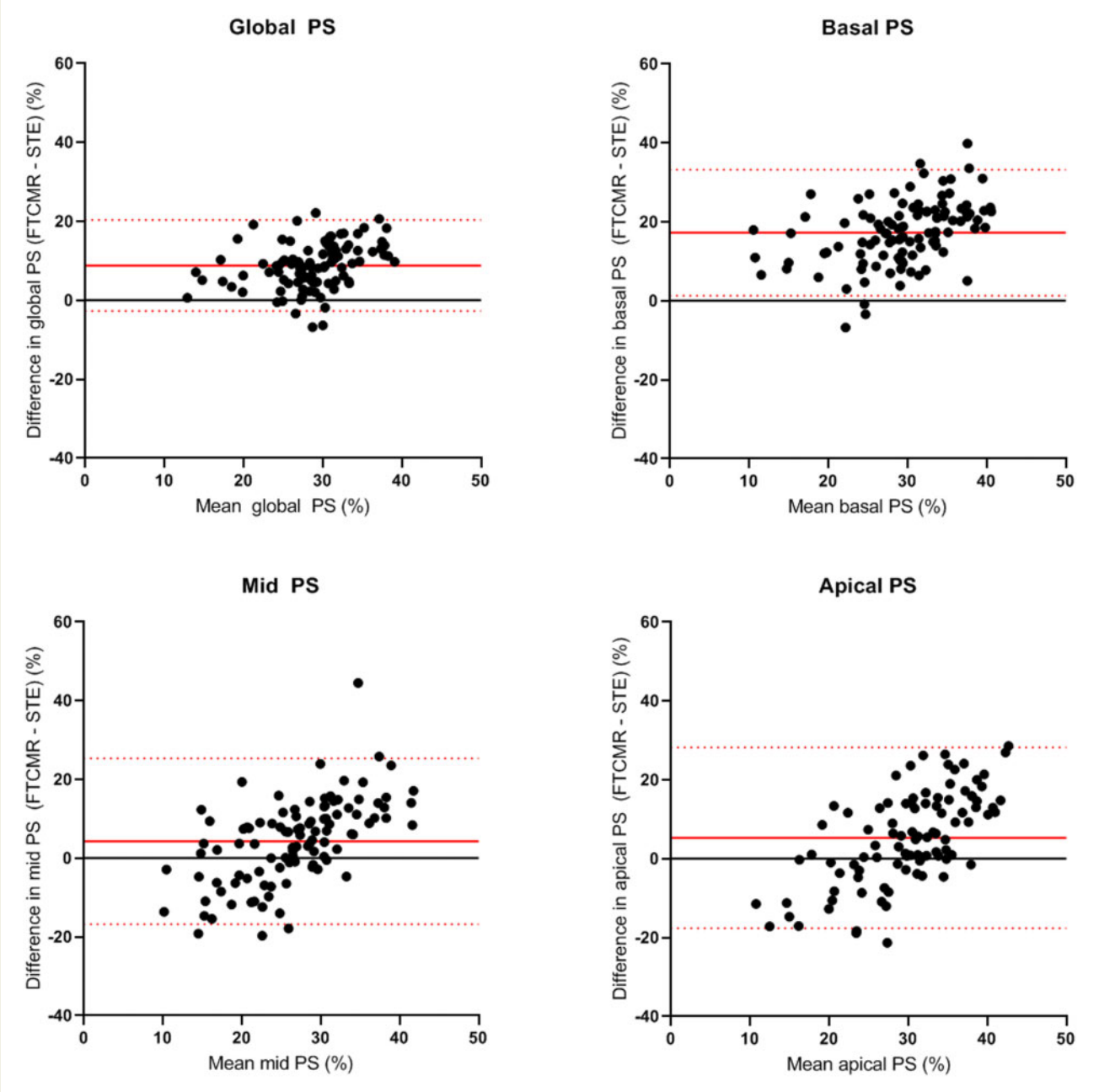

Figure 3 Bland–Altman plots for global and segmental RV PS. Bland–Altman plots show weak agreement between STE and FT-CMR. Agreement is best for global RV PS (upper left plot) and becomes worse when performing regional analysis. FT-CMR, feature tracking cardiovascular magnetic resonance imaging; PS, peak strain; STE, speckle tracking echocardiography.

in the present study. On the other hand, the temporal resolution is higher in echocardiography, which is considered to be beneficial for deformation imaging.[1] This may be a more important factor in the quantification of RV deformation values due to the higher velocities of the RV free wall compared to the LV myocardial velocities (in particular the RV basal segment).[27] Whether this impacts the feature tracking algorithm is unknown.

- The reference method for defining onset of systole was different between STE and FT-CMR in this study. While the timing of these events was ECG-gated with STE, FT-CMR algorithms use ventricular volumes to determine the timing. These differences in timing may have also contributed to the differences in strain values, although the absolute effect of this difference will not explain the mean bias observed in our study.

Future directions

Future studies should be of a longitudinal design to compare the added prognostic values of both techniques. In our study, we only investigated RV PS, because other RV measurements derived by STE (e.g. systolic PS, post-systolic shortening, electromechanical interval, mechanical dispersion) have not been applied in FT-CMR yet.[3,5–7,28] Future studies comparing other RV parameters between STE and FT-CMR may lead to an improvement of agreement and correlation between these techniques. Furthermore, we did not include septal segments in our study because these segments are also part of the LV. Future studies including these segments would also be of interest.

Limitations

The relatively small number of patients that is included in this study might be a potential limitation. However, regarding the magnitude of the differences that were observed between the techniques, we assume that a larger study population will not improve inter-modality agreement to such an extent that the measurements can be used interchangeably.

We included patients only when at least one of the segments of the RV was eligible for strain analysis by both echocardiography and CMR. Therefore, the feasibility of these techniques may be overestimated in this study.

Not all the echocardiograms and CMRs in this study were performed on the same day. Since strain values may be affected by physiological differences (such as heart-rate and loading conditions), this 1-month timeframe may have also induced some differences between the modalities. Nevertheless, more than half of our population had both examinations within 1 day. In addition, a subgroup analysis within this group showed no improvement of correlation and agreement.

Different software packages were used for STE and FT-CMR in this study. To exclude major differences induced by software-variability, we conducted an additional analysis with a similar software package for both techniques that showed no improvement in agreement and correlation. This, in combination with our extensive experience with these particular software packages and the resemblance of regular clinical practice makes the use of different software packages in this study reasonable.

Conclusion

STE and FT-CMR both show a similar trend within the spectrum of ARVC and have a significant correlation regarding RV strain measurements. Inter-modality agreement is however suboptimal, in particular for regional assessment. STE and FT-CMR may therefore both individually have added value for assessment of RV function, but the strain values obtained by these techniques cannot be used interchangeably in clinical practice. Future studies should aim to compare the prognostic values of both techniques.

Supplementary data

Supplementary data are available at *European Heart Journal - Cardiovascular Imaging* online.

Funding

This work is supported by the Dutch Heart Foundation (CVON2015-12 eDETECT). M.B. is supported by the Alexandre Suerman Stipend of the UMC Utrecht (2017). A.S.J.M.t.R. is supported by the Dutch Heart Foundation (2015T058). F.W.A. is supported by UCL Hospitals NIHR Biomedical Research Centre.

Conflict of interest: none declared.

References

1. Amzulescu MS, De Craene M, Langet H, Pasquet A, Vancraeynest D, Pouleur AC *et al.* Myocardial strain imaging: review of general principles, validation, and sources of discrepancies. *Eur Heart J Cardiovasc Imaging* 2019;**20**:605–19.
2. Haugaa KH, Basso C, Badano LP, Bucciarelli-Ducci C, Cardim N, Gaemperli O *et al.*; EACVI Scientific Documents Committee, EACVI Board members and external reviewers; EACVI Scientific Documents Committee, EACVI Board members and external reviewers. Comprehensive multi-modality imaging approach in arrhythmogenic cardiomyopathy-an expert consensus document of the European Association of Cardiovascular Imaging. *Eur Heart J Cardiovasc Imaging* 2017;**18**:237–53.
3. Taha K, Mast TP, Cramer MJ, van der Heijden JF, Asselbergs FW, Doevendans PA *et al.* Evaluation of disease progression in arrhythmogenic cardiomyopathy: the change of echocardiographic deformation characteristics over time. *JACC Cardiovasc Imaging* 2020;**13**:631–4.
4. Bourfiss M, Vigneault DM, Aliyari Ghasebeh M, Murray B, James CA, Tichnell C *et al.* Feature tracking CMR reveals abnormal strain in preclinical arrhythmogenic right ventricular dysplasia/cardiomyopathy: a multisoftware feasibility and clinical implementation study. *J Cardiovasc Magn Reson* 2017;**19**:66.
5. Mast TP, Taha K, Cramer MJ, Lumens J, van der Heijden JF, Bouma BJ *et al.* The prognostic value of right ventricular deformation imaging in early arrhythmogenic right ventricular cardiomyopathy. *JACC Cardiovasc Imaging* 2019;**12**:446–55.
6. Mast TP, Teske AJ, Walmsley J, van der Heijden JF, van Es R, Prinzen FW *et al.* Right ventricular imaging and computer simulation for electromechanical substrate characterization in arrhythmogenic right ventricular cardiomyopathy. *J Am Coll Cardiol* 2016;**68**:2185–97.
7. Mast TP, Teske AJ, Te Riele AS, Groeneweg JA, van der Heijden JF, Velthuis BK *et al.* Prolonged electromechanical interval unmasks arrhythmogenic right ventricular dysplasia/cardiomyopathy in the subclinical stage. *J Cardiovasc Electrophysiol* 2016;**27**:303–14.
8. Heermann P, Hedderich DM, Paul M, Schülke C, Kroeger JR, Baeßler B *et al.* Biventricular myocardial strain analysis in patients with arrhythmogenic right ventricular cardiomyopathy (ARVC) using cardiovascular magnetic resonance feature tracking. *J Cardiovasc Magn Reson* 2014;**16**:75.
9. Vigneault DM, Te Riele A, James CA, Zimmerman SL, Selwaness M, Murray B *et al.* Right ventricular strain by MR quantitatively identifies regional dysfunction in patients with arrhythmogenic right ventricular cardiomyopathy. *J Magn Reson Imaging* 2016;**43**:1132–9.
10. Houard L, Benaets M-B, de Ravenstein de MC, Rousseau MF, Ahn SA, Amzulescu M-S *et al.* Additional prognostic value of 2D right ventricular speckle-tracking strain for prediction of survival in heart failure and reduced ejection fraction. *JACC Cardiovasc Imaging* 2019;**12**:2373–85.
11. Tong X, Poon J, Li A, Kit C, Yamada A, Shiino K *et al.* Validation of cardiac magnetic resonance tissue tracking in the rapid assessment of RV function: a comparative study to echocardiography. *Clin Radiol* 2018;**73**:324.e9–18.
12. Kempny A, Fernandez-Jimenez R, Orwat S, Schuler P, Bunck AC, Maintz D *et al.* Quantification of biventricular myocardial function using cardiac magnetic resonance feature tracking, endocardial border delineation and echocardiographic speckle tracking in patients with repaired tetralogy of Fallot and healthy controls. *J Cardiovasc Magn Reson* 2012;**14**:32.
13. Padiyath A, Gribben P, Abraham JR, Li L, Rangamani S, Schuster A *et al.* Echocardiography and cardiac magnetic resonance-based feature tracking in the assessment of myocardial mechanics in tetralogy of fallot: an intermodality comparison. *Echocardiography* 2013;**30**:203–10.
14. Corrado D, Link MS, Calkins H. Arrhythmogenic right ventricular cardiomyopathy. *N Engl J Med* 2017;**376**:61–72.
15. Corrado D, Wichter T, Link MS, Hauer RNW, Marchlinski FE, Anastasakis A *et al.* Treatment of arrhythmogenic right ventricular cardiomyopathy/dysplasia: an International Task Force Consensus Statement. *Circulation* 2015;**132**:441–53.
16. Obokata M, Nagata Y, Wu V-C, Kado Y, Kurabayashi M, Otsuji Y *et al.* Direct comparison of cardiac magnetic resonance feature tracking and 2D/3D echocardiography speckle tracking for evaluation of global left ventricular strain. *Eur Heart J Cardiovasc Imaging* 2016;**17**:525–32.

17. Aurich M, Keller M, Greiner S, Steen H, Aus Dem Siepen F, Riffel J *et al*. Left ventricular mechanics assessed by two-dimensional echocardiography and cardiac magnetic resonance imaging: comparison of high-resolution speckle tracking and feature tracking. *Eur Heart J Cardiovasc Imaging* 2016;**17**:1370–8.
18. van Everdingen WM, Zweerink A, Nijveldt R, Salden OAE, Meine M, Maass AH *et al*. Comparison of strain imaging techniques in CRT candidates: CMR tagging, CMR feature tracking and speckle tracking echocardiography. *Int J Cardiovasc Imaging* 2018;**34**:443–56.
19. Marcus FI, McKenna WJ, Sherrill D, Basso C, Bauce B, Bluemke DA *et al*. Diagnosis of arrhythmogenic right ventricular cardiomyopathy/dysplasia: proposed modification of the task force criteria. *Circulation* 2010;**121**:1533–41.
20. Bosman LP, Verstraelen TE, van Lint FHM, Cox M, Groeneweg JA, Mast TP *et al*.; Netherlands ACM Registry. The Netherlands Arrhythmogenic Cardiomyopathy Registry: design and status update. *Neth Heart J* 2019;**27**:480–6.
21. Teske AJ, Prakken NH, De Boeck BW, Velthuis BK, Martens EP, Doevendans PA *et al*. Echocardiographic tissue deformation imaging of right ventricular systolic function in endurance athletes. *Eur Heart J* 2008;**30**:969–77.
22. Teske AJ, De Boeck BWL, Melman PG, Sieswerda GT, Doevendans PA, Cramer M. Echocardiographic quantification of myocardial function using tissue deformation imaging, a guide to image acquisition and analysis using tissue Doppler and speckle tracking. *Cardiovasc Ultrasound* 2007;**5**:27.
23. Badano LP, Kolias TJ, Muraru D, Abraham TP, Aurigemma G, Edvardsen T *et al*.; Industry representatives; Reviewers: This document was reviewed by members of the 2016–2018 EACVI Scientific Documents Committee. Standardization of left atrial, right ventricular, and right atrial deformation imaging using two-dimensional speckle tracking echocardiography: a consensus document of the EACVI/ASE/Industry Task Force to standardize deformation imaging. *Eur Heart J Cardiovasc Imaging* 2018;**19**:591–600.
24. Kawel-Boehm N, Maceira A, Valsangiacomo-Buechel ER, Vogel-Claussen J, Turkbey EB, Williams R *et al*. Normal values for cardiovascular magnetic resonance in adults and children. *J Cardiovasc Magn Reson* 2015;**17**:29.
25. Atsumi A, Seo Y, Ishizu T, Nakamura A, Enomoto Y, Harimura Y *et al*. Right ventricular deformation analyses using a three-dimensional speckle-tracking echocardiographic system specialized for the right ventricle. *J Am Soc Echocardiogr* 2016;**29**:402–11.e2.
26. Chen R, Zhu M, Amacher K, Wu X, Sahn DJ, Ashraf M. Non-invasive evaluation of right ventricular function with real-time 3-D echocardiography. *Ultrasound Med Biol* 2017;**43**:2247–55.
27. Caballero L, Kou S, Dulgheru R, Gonjilashvili N, Athanassopoulos GD, Barone D *et al*. Echocardiographic reference ranges for normal cardiac Doppler data: results from the NORRE Study. *Eur Heart J Cardiovasc Imaging* 2015;**16**:1031–41.
28. Sarvari SI, Haugaa KH, Anfinsen O-G, Leren TP, Smiseth OA, Kongsgaard E *et al*. Right ventricular mechanical dispersion is related to malignant arrhythmias: a study of patients with arrhythmogenic right ventricular cardiomyopathy and subclinical right ventricular dysfunction. *Eur Heart J* 2011;**32**:1089–96.